

# Involvement of the GluN2A and GluN2B Subunits in Synaptic and Extrasynaptic *N*-methyl-D-aspartate Receptor Function and Neuronal Excitotoxicity\*

Received for publication, April 30, 2013, and in revised form, June 26, 2013. Published, JBC Papers in Press, July 9, 2013, DOI 10.1074/jbc.M113.482000

Xianju Zhou<sup>‡§¶1</sup>, Qi Ding<sup>‡</sup>, Zhuoyou Chen<sup>¶</sup>, Huifang Yun<sup>¶</sup>, and Hongbing Wang<sup>‡§2</sup>

From the <sup>‡</sup>Department of Physiology, <sup>§</sup>Neuroscience Program, Michigan State University, East Lansing, Michigan 48824, the

<sup>¶</sup>Department of Neurology, <sup>||</sup>Department of Anesthesiology, Changzhou No. 2 People's Hospital, The Affiliated Hospital of Nanjing Medical University, 29 Xinglong Alley, Changzhou 213003, China

**Background:** The function of NMDAR subtypes in neuronal signaling and excitotoxicity remains unclear.

**Results:** GluN2A and GluN2B regulate both synaptic and extrasynaptic signaling and contribute to excitotoxicity.

**Conclusion:** GluN2A and GluN2B play similar rather than opposing roles in NMDAR-mediated signaling and excitotoxicity.

**Significance:** Knowing the function of NMDAR subtypes is critical for understanding how neuronal fate is regulated.

GluN2A and GluN2B are the major subunits of functional NMDA receptors (NMDAR). Previous studies have suggested that GluN2A and GluN2B may differentially mediate NMDAR function at synaptic and extrasynaptic locations and play opposing roles in excitotoxicity, such as neurodegeneration triggered by ischemic stroke and brain injury. By using pharmacological and molecular approaches to suppress or enhance the function of GluN2A and GluN2B in cultured cortical neurons, we examined NMDAR-mediated, bidirectional regulation of prosurvival signaling (*i.e.* the cAMP response element-binding protein (CREB)-*Bdnf* cascade) and cell death. Inhibition of GluN2A or GluN2B attenuated the up-regulation of prosurvival signaling triggered by the activation of either synaptic or extrasynaptic NMDAR. Inhibition of GluN2A or GluN2B also attenuated the down-regulation of prosurvival signaling triggered by the coactivation of synaptic and extrasynaptic receptors. The effects of GluN2B on CREB-*Bdnf* signaling were larger than those of GluN2A. Consistently, compared with suppression of GluN2A, suppression of GluN2B resulted in more reduction of NMDA- and oxygen glucose deprivation-induced excitotoxicity as well as NMDAR-mediated elevation of intracellular calcium. Moreover, excitotoxicity and down-regulation of CREB were exaggerated in neurons overexpressing GluN2A or GluN2B. Together, we found that GluN2A and GluN2B are involved in the function of both synaptic and extrasynaptic NMDAR, demonstrating that they play similar rather than opposing roles in NMDAR-mediated bidirectional regulation of prosurvival signaling and neuronal death.

Glutamate mediates the majority of excitatory neurotransmission in the central nervous system. Among the identified ionotropic glutamate receptors, the *N*-methyl-D-aspartate receptors (NMDARs)<sup>3</sup> are particularly highly permeable to Ca<sup>2+</sup> (1). Excessive activation of NMDAR under pathological conditions results in excitotoxicity, such as neurodegeneration following ischemic stroke (2). However, because appropriate NMDAR activation is pivotal for neuronal development and survival (3–5), global inhibition of NMDAR fails to effectively attenuate excitotoxicity caused by cerebral ischemia (6). Thus, recent therapeutic development has focused on blocking subtypes (7, 8) or subpopulations of NMDAR (9) to achieve neuroprotective effects.

The tetrameric NMDAR is comprised of two essential GluN1 subunits and two GluN2 subunits or the relatively rare GluN3 subunits (1). The essential function of the GluN1 subunit is implicated by the lack of intact synaptic plasticity or neurotoxicity in GluN1 mutant neurons (10). GluN1 knockout mice are also perinatal lethal, suggesting its function in development and survival. In the adult forebrain, GluN2A and GluN2B subunits are the predominant GluN2 subunits (11). There is reasonable evidence showing that GluN2A and GluN2B are present at both synaptic and extrasynaptic locations (12, 13). However, it is not clear whether they are both involved in the survival- or death-related intracellular signaling triggered by the activation of synaptic or extrasynaptic NMDAR (syn- or ex-NMDAR). Because of the different characteristics of the GluN2A and GluN2B subunits, such as channel kinetics and their distinct interaction with different signaling molecules (1, 14), it is tempting to speculate that these two NMDAR subtypes have distinct functions. Indeed, it has been proposed that activation of GluN2A and

\* This work was supported, in whole or in part, by National Institutes of Health Grants MH093445 and NS072668. This work was also supported by American Heart Association Postdoctoral Fellowship 10POST4450000.

<sup>1</sup> To whom correspondence may be addressed: Department of Neurology, Changzhou No.2 People's Hospital, 29 Xinglong Alley, Changzhou 213003, China. Tel.: 86-81087079; Fax: 86-519-81087711; E-mail: hippocampus2007@gmail.com.

<sup>2</sup> To whom correspondence may be addressed: 567 Wilson Rd., Room 3179, Biomedical and Physical Sciences Building, Michigan State University, East Lansing, MI 48824. Tel.: 517-884-5119; Fax: 517-355-5125; E-mail: wangho@msu.edu.

<sup>3</sup> The abbreviations used are: NMDAR, NMDA receptor; syn-NMDAR, synaptic NMDA receptor; ex-NMDAR, extrasynaptic NMDA receptor; CREB, cAMP response element-binding protein; L-VGCC, L-type voltage-gated calcium channel; p-CREB, cAMP response element-binding protein phosphorylation; OGD, oxygen-glucose deprivation; DIV, days *in vitro*; ANOVA, analysis of variance; SNK, Student-Newman-Keuls; CNQX, 6-cyano-7-nitroquinoxaline-2,3-dione; NVP-AAM077, [(R)-[(S)-1-(4-bromophenyl)-ethylamino]-2,3-dioxo-1,2,3,4-tetrahydroquinoxalin-5-yl]-methyl]-phosphonic acid.

GluN2B stimulates different signaling cascades (15, 16) and regulates survival and excitotoxicity, respectively (7, 8).

Our previous study (17) shows how NMDAR bidirectionally regulates cell survival and death. Specifically, we demonstrated that the prosurvival CREB (cAMP response element-binding protein) signaling is up-regulated by the activation of either syn- or ex-NMDAR. Coactivation of syn- and ex-NMDAR triggers cell death and dampens CREB signaling (17). Here we demonstrate that both GluN2A and GluN2B are involved in syn- as well as ex-NMDAR function. Suppression of either GluN2A or GluN2B dampened NMDAR-mediated cell death. However, compared with GluN2A, GluN2B had a larger impact on both NMDAR-mediated intracellular signaling and cell death.

### EXPERIMENTAL PROCEDURES

**Primary Culture of Cortical Neurons**—The experimental procedures were in accordance with the animal welfare guidelines and approved by the Institutional Animal Care and Use Committee at Michigan State University. Cortices were obtained from postnatal day 0 Sprague-Dawley rats, dissociated, and used for the primary culture as described in our previous study (17).

**Neuronal Stimulation**—To activate NMDARs, neurons were stimulated with NMDA (at 15, 30, 50, and 100  $\mu\text{M}$  as indicated for each individual experiment) or bicuculline (50  $\mu\text{M}$ , Sigma) along with the NMDAR coagonist glycine (at 2  $\mu\text{M}$ ). In all experiments, except the ones in Fig. 4C, a 30-min pretreatment with nifedipine (5  $\mu\text{M}$ , Sigma) and 6-cyano-7-nitroquinoxaline-2,3-dione (CNQX) (20  $\mu\text{M}$ , Sigma) were applied to block L-type voltage-gated calcium channels (L-VGCCs) and non-NMDA type glutamate receptors, respectively. A 30-min pretreatment with NVP-AAM077 (a gift from Dr. Yves P. Auberson, Novartis Institutes of Biomedical Research, Switzerland) and ifenprodil (3  $\mu\text{M}$ , Sigma) was used to inhibit GluN2A and GluN2B, respectively.

**Western Blot Analysis and Semiquantitative RT-PCR**—The activation of CREB was determined by the level of CREB phosphorylation (p-CREB) at Ser-133 with Western blot analysis as described (17). The NMDAR-mediated transcription of *Bdnf* was determined by semiquantitative RT-PCR (18).

**Induction and Assessment of Neuronal Death**—Neurons were treated with NMDA (30, 50, and 100  $\mu\text{M}$  as indicated for each individual experiment) and 2  $\mu\text{M}$  glycine with or without (for the experiment in Fig. 4C2) CNQX (20  $\mu\text{M}$ ), and nifedipine (5  $\mu\text{M}$ ) for 20 or 30 min (as indicated), followed by a wash with conditioned medium. The neurons were retained in mixed medium containing 50% conditioned medium and 50% fresh medium for 20 h and then stained with DAPI (1  $\mu\text{g}/\text{ml}$ ). We also included 1  $\mu\text{M}$  MK801 during the 20-hour post-treatment incubation so that the activation of NMDAR because of excessive glutamate release from the dying neurons could be suppressed. The appearance of condensed nuclear (or condensed chromatin) staining (revealed by DAPI) were used as an indicator for cell death as described in previous studies (19, 20).

To mimic ischemic stroke *in vitro*, we subjected neurons to oxygen-glucose deprivation (OGD) (21). As described in our previous study (17), neurons were incubated in glucose-free solution and exposed to 95% N<sub>2</sub> and 5% CO<sub>2</sub> in a hypoxia

chamber (Billups-Rothenberg, Inc.) for 65 min. OGD was then terminated, and cell death was determined by DAPI staining 20 h later.

Additionally, the formation of dendritic varicosity and cell body swelling were examined as early cellular signs of cell death (22). Neurons were first transfected with cDNA expressing GFP. Before NMDA treatment, 150 GFP-labeled neurons were chosen randomly from six areas and examined. Following NMDA treatment for 30 min, neurons with at least one dendritic varicosity were counted as damaged cells. Under our experimental conditions, most neurons that underwent dendritic morphological changes showed more than five varicosities. As an alternative and an additional measurement of cell death, the percentage of neurons showing cell body swelling was also analyzed. The cell body images of the same GFP-positive neurons before and after NMDA treatment were compared to determine NMDA-induced cell body swelling.

**Calcium Imaging**—The NMDAR-mediated changes in intracellular calcium ( $\text{Ca}^{2+}_i$ ) level were determined in live neurons by calcium imaging (17). The ratio of fluorescent emission (fura-2 emission at 520 nm) excited by 340 nm and 380 nm was used to determine the relative  $\text{Ca}^{2+}_i$  level.

**Overexpression and shRNA-mediated Knockdown of GluN2A and GluN2B**—We used two independent shRNA constructs to effectively knock down GluN2A and GluN2B, as described in our previous study (23). For the knockdown experiments, a GFP plasmid (0.5  $\mu\text{g}$ ) along with one of the target shRNA constructs or scrambled shRNA construct were cotransfected into DIV (days *in vitro*) 16 neurons using the Lipofectamine<sup>TM</sup> method (Invitrogen). The transfected neurons were stimulated by NMDA on DIV 21, and the level of NMDA-mediated phosphorylation of CREB and neuronal death were examined by immunofluorescent staining.

To overexpress GluN2A or GluN2B subunits, neurons at DIV 7 were transfected with 1  $\mu\text{g}$  of cDNA construct expressing GFP-GluN2A or GFP-GluN2B (24) (gifts from Dr. Katherine Roche at the National Institute of Neurological Disorders and Stroke). The effects of GluN2 overexpression on NMDA-mediated CREB phosphorylation and neuronal death were examined 2 days after transfection.

**Fluorescent Immunostaining**—Following NMDA treatment, neurons were fixed with 4% paraformaldehyde and 4% sucrose in PBS for 10 min at room temperature and then rinsed three times with PBS. After a 1-h incubation with 10% normal goat serum (Invitrogen) in PBS-T (PBS containing 0.1% Triton X-100), the fixed neurons were incubated with primary antibody against p-CREB at Ser-133 (1:1000) overnight. The secondary antibody (Alexa Fluor 594-conjugated goat anti-rabbit IgG, 1:1000, Invitrogen) was incubated at room temperature for 1 h. To obtain a GFP signal, Alexa Fluor 488-conjugated anti-GFP (1:1000, Invitrogen) was subsequently incubated for 1 h at room temperature. A Nikon fluorescence microscope was used for imaging. Quantification was performed by analyzing the fluorescence intensity of p-CREB using ImageJ and presented as mean  $\pm$  S.E.

**Data Analysis**—Results from multiple repeats are expressed as mean  $\pm$  S.E. The statistical significance analysis for the difference among multiple groups/treatments was performed

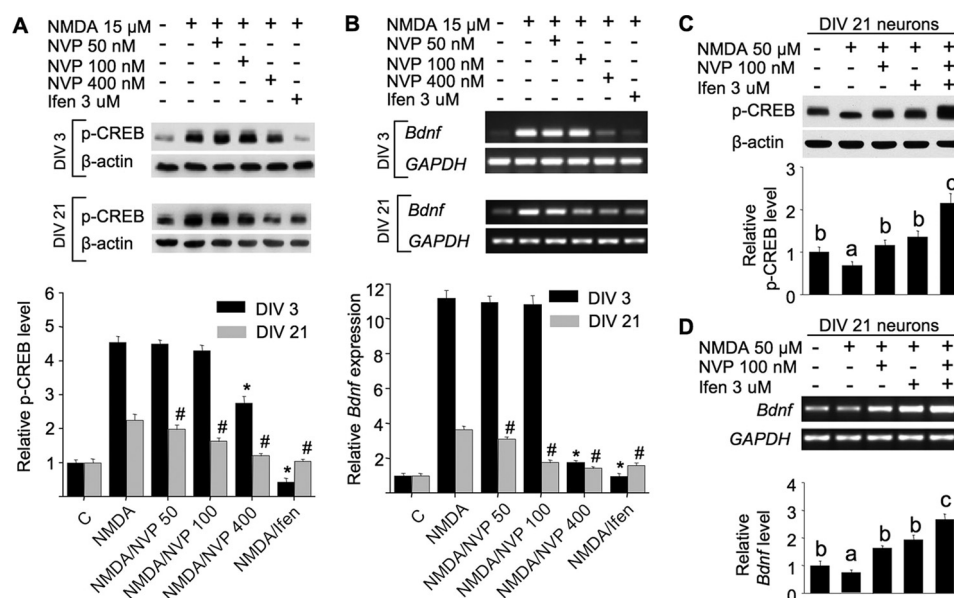


**FIGURE 1. Bidirectional regulation of the CREB-Bdnf cascade by NMDAR requires both GluN2A and GluN2B.** DIV 3 (A and B) or DIV 21 (A–D) neurons were pretreated with NVP-AAM077 (NVP, 50, 100, or 400 nM as indicated), ifenprodil (Ifen, 3  $\mu$ M), or both, followed by NMDA (15 or 50  $\mu$ M, as indicated) stimulation (along with 2  $\mu$ M NMDAR coagonist glycine). A 30-min pretreatment with 5  $\mu$ M nifedipine and 20  $\mu$ M CNQX was included to block L-VGCCs and non-NMDA-type glutamate receptors, respectively. A and C, 15 min after NMDA stimulation, cell lysates were analyzed for the level of CREB phosphorylation at Ser-133 (p-CREB) by Western blot analysis. The level of  $\beta$ -actin was used as a loading control. B and D, 1 h after NMDA stimulation, the level of *Bdnf* mRNA was determined by semiquantitative RT-PCR. *GAPDH* was used as an internal control. \* and #,  $p < 0.05$  compared with NMDA-treated samples. C and D, one-way ANOVA revealed a significant difference (i.e.  $p < 0.05$ ) among different treatments. The post hoc SNK analysis revealed that the values associated with distinct SNK groups (a, b, and c) are significantly different:  $a < b < c$ .

with one-way ANOVA. Following ANOVA, post hoc Student-Newman-Keuls (SNK) procedure was used to determine whether the data are statistically different from each other. Data between two groups were analyzed by the Student's  $t$  test.

## RESULTS

**Both GluN2A and GluN2B Are Involved in NMDAR-mediated Bidirectional Regulation of the CREB-Bdnf Signaling Cascade**—Numerous studies have demonstrated that appropriate activation of NMDAR activates prosurvival molecules (such as CREB) and supports neuronal survival (17, 25–27). NMDAR overactivation results in significant cell death. Consistent with our recent study (17), low-dose NMDA at 15  $\mu$ M activated CREB (Fig. 1A) and up-regulated the transcription of a CREB target gene, *Bdnf* (Fig. 1B). Conversely, high-dose NMDA at 50  $\mu$ M down-regulated CREB activity (Fig. 1C) and *Bdnf* transcription (Fig. 1D).

The GluN2A and GluN2B subunits are the predominant GluN2 subunits in the forebrain regions. To determine their function in NMDAR-mediated CREB-Bdnf signaling, we chose to use selective inhibitors for these GluN2 subunits. Although the selectivity of ifenprodil for GluN2B is well accepted, the selectivity of NVP-AAM077 for GluN2A over GluN2B is concentration-dependent (28, 29). To determine the dose of NVP-AAM077 that has significant GluN2A selectivity, we examined the effects of NVP-AAM077 on DIV 3 and DIV 21 neurons. Previous studies (30, 31), including ours (32), have shown that GluN2A expression is regulated developmentally. Specifically, we found that the expression level of GluN2B in cultured cortical neurons is relatively constant from DIV 3 to DIV 22. In contrast, the expression of GluN2A is undetectable on DIV 3,

emerges on DIV 13, and is increased further along with *in vitro* neuronal maturation after 3 weeks of culturing (32). Here, we found that the NMDA-activated (15  $\mu$ M) CREB phosphorylation and *Bdnf* transcription were suppressed significantly by ifenprodil in both DIV 3 and DIV 21 neurons (Fig. 1, A and B). The effects of NVP-AAM077 were regulated developmentally. NVP-AAM077 at 100 and 400 nM showed suppression effects in DIV 21 neurons. The suppression effects were only observed with 400 but not 100 nM NVP-AAM077 in DIV 3 neurons (Fig. 1, A and B). Because DIV 3 neurons do not express GluN2A, these data imply that 100 nM NVP-AAM077 predominantly inhibits GluN2A without significantly inhibiting the GluN2B-containing receptors and that 400 nM non-specifically inhibits both GluN2A and GluN2B. The concentration-dependent selectivity of NVP-AAM077 is consistent with the findings from previous studies (28, 29). Thus, we examined DIV 21 neurons and used 100 nM NVP-AAM077 to block GluN2A for all later experiments. We next found that blocking either GluN2A or GluN2B significantly rescued CREB deactivation (Fig. 1C) and *Bdnf* down-regulation (Fig. 1D), which were triggered by high NMDA at 50  $\mu$ M.

**Both the GluN2A and GluN2B Subunits Are Involved in Intracellular Signaling Triggered by the Activation of Syn-NMDAR or Ex-NMDAR**—It is known that activation of syn-NMDAR up-regulates CREB, whose activation supports neuronal survival (9). Here we confirmed that bicuculline, which causes presynaptic disinhibition and triggers the presynaptic release of glutamate leading to syn-NMDAR activation, significantly up-regulated CREB activity and *Bdnf* transcription (Fig. 2, A and B). These increases were dampened by either 100 nM NVP-AAM077 or ifenprodil. Coapplication of NVP-AAM077



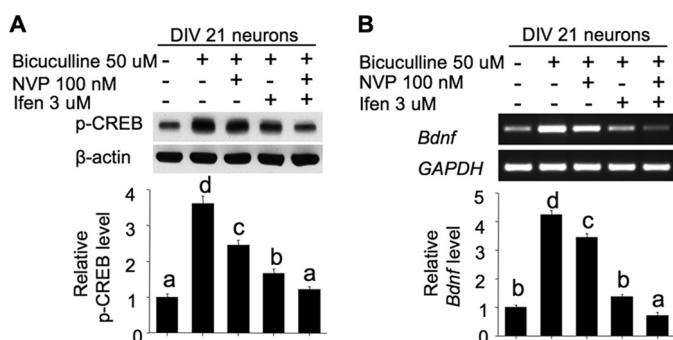


**FIGURE 2. Both GluN2A- and GluN2B-containing NMDARs are involved in intracellular responses triggered by synaptic receptor activation.** DIV 21 neurons were stimulated with bicuculline (50  $\mu$ M) along with 2  $\mu$ M glycine, 5  $\mu$ M nifedipine, and 20  $\mu$ M CNQX for 15 min (A) or 1 h (B) following a 30-min pretreatment with NVP-AAM077 (NVP, 100 nM) or ifenprodil (Ifen, 3  $\mu$ M) as indicated. The level of p-CREB (A) and *Bdnf* mRNA (B) were examined by Western blot analysis and RT-PCR, respectively. One-way ANOVA revealed a significant difference (*i.e.*  $p < 0.05$ ) among different treatments. The post hoc SNK analysis revealed that the values associated with distinct SNK groups (a, b, c, and d) are significantly different:  $a < b < c < d$ .

and ifenprodil achieved complete inhibition of p-CREB and *Bdnf* transcription (Fig. 2, A and B).

Our recent study showed that, although coactivation of syn- and ex-NMDAR leads to deactivation of prosurvival signaling and triggers cell death, activation of ex-NMDAR alone stimulates the CREB-*Bdnf* cascade (17). We used a well accepted method to activate ex-NMDAR. We first pretreated neurons with bicuculline and MK801 for 2 min, followed by a wash and subsequent incubation with 50  $\mu$ M NMDA (17). Because bicuculline selectively activates syn-NMDAR and MK801 irreversibly blocks opened NMDAR, pretreating neurons with bicuculline and MK801-blocked syn-NMDAR and the subsequent application of 50  $\mu$ M NMDA only activated the available ex-NMDAR. Here we reconfirmed that activation of ex-NMDAR caused an increase in p-CREB (Fig. 3A) and *Bdnf* mRNA (Fig. 3B). The up-regulation was significantly suppressed by either NVP-AAM077 or ifenprodil (Fig. 3, A and B). Coapplication of these inhibitors completely suppressed the intracellular responses triggered by ex-NMDAR (Fig. 3, A and B).

Together, these results suggest that both the GluN2A and GluN2B subunits are required for NMDAR function at either synaptic or extrasynaptic sites. It is important to emphasize that blocking GluN2B had greater effects than blocking GluN2A.

**Both the GluN2A and GluN2B Subunits Are Involved in the NMDAR-mediated Excitotoxicity**—It has been shown that, compared with proper activation of NMDAR under physiological conditions, overactivation of NMDAR shuts off the prosurvival signaling and, in turn, triggers cell death (2, 33, 34). In contrast to neurons stimulated with bicuculline or 15  $\mu$ M NMDA, 50  $\mu$ M NMDA dephosphorylated CREB and down-regulated *Bdnf* transcription (Fig. 1, C and D). NMDA at 50  $\mu$ M triggered significant cell death (43.2% of the DAPI-stained neurons show condensed nuclear staining, Fig. 4A). Neurons pretreated with 100 nM NVP-AAM077 and ifenprodil showed 29.4% and 19.8% death, respectively (Fig. 4A). Coapplication of the two antagonists completely blocked NMDA-induced neuronal death triggered by 50  $\mu$ M NMDA (Fig. 4A). These data demonstrate that both GluN2A and GluN2B are involved in

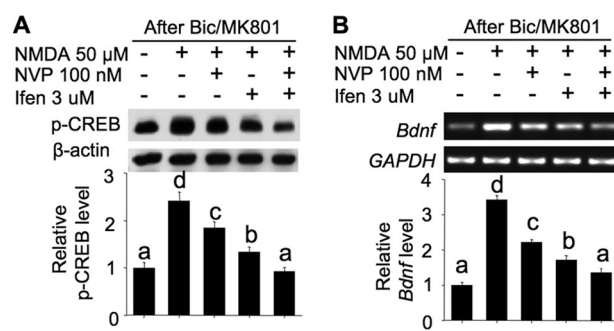


**FIGURE 3. Both GluN2A- and GluN2B-containing NMDARs are involved in intracellular responses triggered by extrasynaptic receptor activation.** To activate ex-NMDAR, DIV 21 neurons were first incubated with bicuculline (Bic, 50  $\mu$ M) and MK801 (10  $\mu$ M) for 2 min, rinsed three times with conditioned medium, and then stimulated with 50  $\mu$ M NMDA for 15 min (A) or 60 min (B). All treatment included the application of 2  $\mu$ M glycine, 5  $\mu$ M nifedipine, and 20  $\mu$ M CNQX. The level of p-CREB (A) and *Bdnf* mRNA (B) was determined. One-way ANOVA revealed a significant difference (*i.e.*  $p < 0.05$ ) among different treatments. The post hoc SNK analysis revealed that the values associated with distinct SNK groups (a, b, c, and d) are significantly different:  $a < b < c < d$ . NVP, NVP-AAM077; Ifen, ifenprodil.

NMDAR-mediated excitotoxicity and that blocking GluN2B renders more protection than blocking GluN2A.

Because the deactivation of prosurvival signaling also depends on the duration of the pathological insults, we treated neurons with 50  $\mu$ M NMDA for a longer period of time (*i.e.* 30 min compared with 15 min in Fig. 1C) and measured the level of p-CREB. Such a stimulation caused a more dramatic deactivation of CREB, which was rescued by ifenprodil but only partially by 100 nM NVP-AAM077 (Fig. 4B). It has been demonstrated that the activation of L-VGCCs (35–37) and non-NMDA-type glutamate receptors (38–40) also contributes to the degree of cell death. We next treated neurons with 50  $\mu$ M NMDA for 30 min without nifedipine and CNQX. Under this condition, ifenprodil dampened the NMDA-triggered CREB dephosphorylation (Fig. 4C1) and cell death (Fig. 4C2). In contrast, 100 nM NVP-AAM077 did not show measurable effects (Fig. 4C). These results show that blocking GluN2A is less effective to attenuate cell death under more severe pathological conditions.

We next determined directly whether the protective effects from blocking GluN2A and 2B depend on the degree of insult caused by NMDAR overactivation. A milder insult by 30  $\mu$ M NMDA caused less cell death, which was completely suppressed by either NVP-AAM077 or ifenprodil (Fig. 4A). A more severe insult by 100  $\mu$ M NMDA caused more cell death, which is only attenuated by ifenprodil but not by NVP-AAM077 (Fig. 4A). Coapplication of NVP-AAM077 and ifenprodil completely blocked death following either 30 or 100  $\mu$ M NMDA (Fig. 4A). These lines of evidence (Figs. 1, C and D, and 4, A, B, and C) demonstrate that, although both GluN2A and 2B are involved in regulating survival and death, GluN2B plays a more dominant role under more severe pathological conditions.

We next subjected neurons to a 65-min OGD that involved NMDAR overactivation. Compared with vehicle controls (70.5% cell death), incubation with 100 nM NVP-AAM077 and ifenprodil during OGD reduced cell death to 49.7 and 31.2%, respectively (Fig. 4D).

Because NMDAR-mediated  $\text{Ca}^{2+}$  overload is directly related to the onset of death (41–43), we postulated that the higher

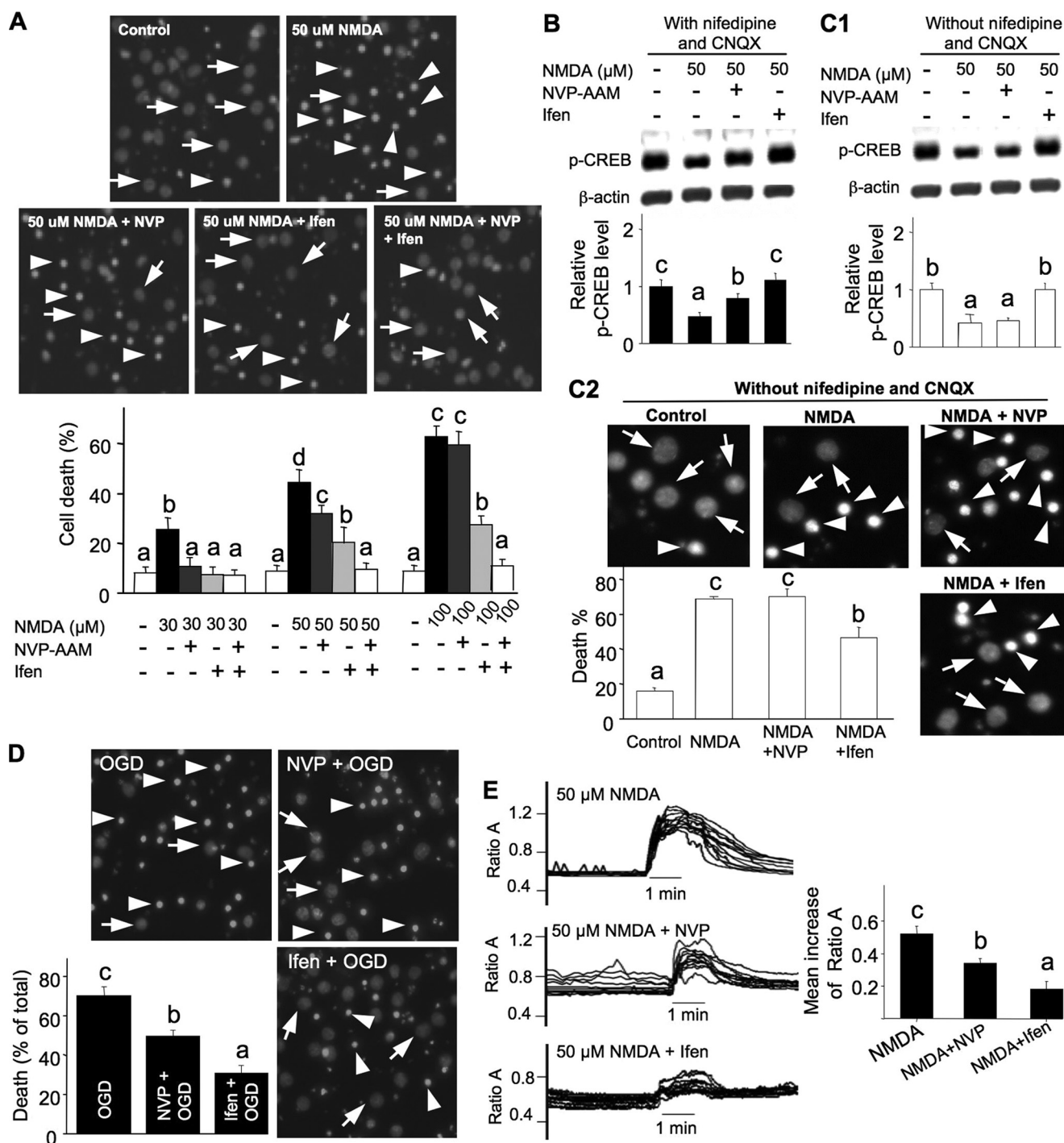


**FIGURE 4. Involvement of GluN2A and GluN2B in NMDA- and OGD-induced cell death.** DIV 21 neurons were first treated with 100 nM NVP-AAM077 (NVP) or 3 μM ifenprodil (Ifen) for 30 min and then subjected to NMDA (30, 50, or 100 μM as indicated) stimulation (A–C and E) or OGD (D). Neuronal death was determined by DAPI staining. The percentage of cells with condensed nuclear staining (arrowheads) increased significantly following NMDA (A and C2) and OGD (D). The healthy cells with diffuse nuclear staining are indicated by arrows. The levels of p-CREB and β-actin were determined by Western blot analysis (B and C1). E, contribution of GluN2A and GluN2B to NMDAR-mediated  $Ca^{2+}$  influx.  $Ca^{2+}$  was determined by calcium imaging following NMDA stimulation in the presence of GluN2A and GluN2B inhibitors. For A, B, and E, treatments included the application of 2 μM glycine, 5 μM nifedipine, and 20 μM CNQX. For C, nifedipine and CNQX were not included. The duration of NMDA treatments was 20 (A), 30 (B and C), and 1 min (E). One-way ANOVA revealed a significant difference (i.e.  $p < 0.05$ ) among different treatments. The post hoc SNK analysis revealed that the values associated with distinct SNK groups (a, b, c, and d) are significantly different:  $a < b < c < d$  (whenever it is applicable for the corresponding data sets).

impact of GluN2B on cell death might be attributed to its contribution to the elevation of intracellular  $Ca^{2+}$ . To investigate this possibility, we examined the relative level of intracellular  $Ca^{2+}$  ( $Ca^{2+}_i$ ) by calcium imaging with live neurons. As expected, the GluN2B antagonist ifenprodil caused more reduction of

NMDAR-mediated  $Ca^{2+}_i$  elevation than the GluN2A antagonist NVP-AAM077 (Fig. 4E).

**Molecular Knockdown of GluN2A and GluN2B Attenuates NMDAR-mediated Neuronal Death**—To further determine the function of GluN2A and GluN2B, we used shRNA-mediated



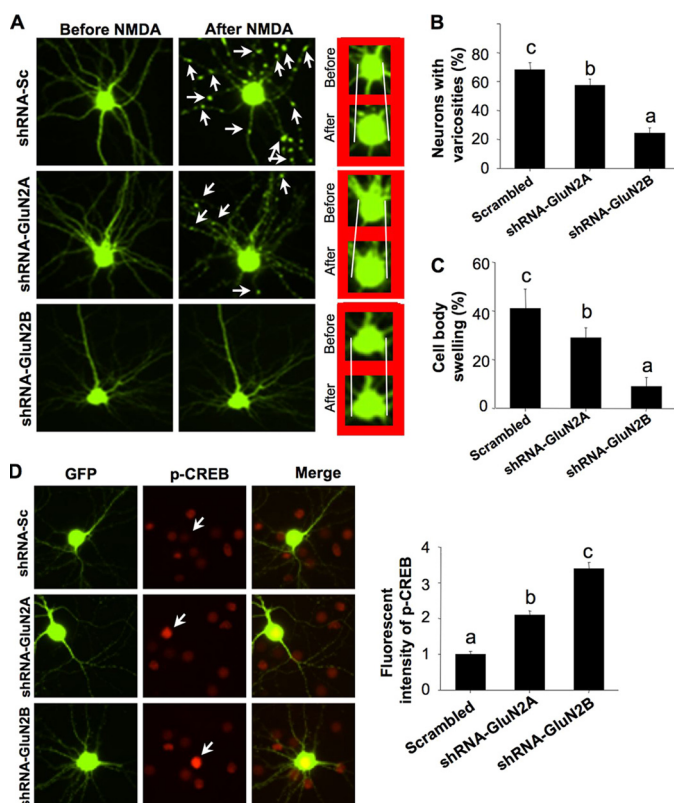


**FIGURE 5. Effects of GluN2A and GluN2B knockdown on NMDAR-mediated excitotoxicity and CREB phosphorylation.** Live neurons cotransfected with GFP and scrambled shRNA (shRNA-Sc) or shRNA-GluN2Aa or shRNA-GluN2Bm were monitored before and after the 30-min NMDA (50  $\mu$ M) treatment (A), which included the application of 2  $\mu$ M glycine, 5  $\mu$ M nifedipine, and 20  $\mu$ M CNQX. Neurons with the formation of varicosity and cell body swelling were counted and quantified (B and C). The images of the same GFP-positive neuron before and after NMDA treatment are shown (A). The multiple varicosities appeared in representative neurons following NMDA treatment (arrows). The cell body of the same neuron before and after NMDA treatment is enlarged and compared in the right panels. Cell body swelling of the representative neurons is indicated by the non-parallel diverging lines. D, transfected neurons were treated with 50  $\mu$ M NMDA for 10 min and then fixed and costained for p-CREB and GFP (D). The relative intensity of the p-CREB signal (as indicated by arrows for the representative GFP-positive cell) in neurons transfected with GFP and scrambled shRNA was defined as 1 (right panel) and compared with those in neurons transfected with GFP and GluN2A or GluN2B shRNA constructs. One-way ANOVA revealed a significant difference (i.e.  $p < 0.05$ ) among different treatments. The post hoc SNK analysis revealed that the values associated with distinct SNK groups (a, b, and c) are significantly different:  $a < b < c$ .

knockdown to suppress the expression of these two genes. We used two different shRNA constructs to knock down either the GluN2A (by shRNA-GluN2Aa and shRNA-GluN2Ac) or GluN2B subunits (by shRNA-GluN2Bm and shRNA-GluN2Bi). Previous studies, including ours, have shown that these shRNAs suppress more than 90% expression of GluN2A and GluN2B, respectively (23, 44). Here we observed that a 30-min treatment with 50  $\mu$ M NMDA induced a remarkable appearance of dendritic varicosity and cell body swelling, which are well characterized cellular signs of NMDAR-mediated excitotoxicity (22). Knockdown of GluN2A expression by shRNA-GluN2Aa led to a mild but significant decrease in the percentage of neurons with dendritic varicosities (Fig. 5A, center panel, arrows) and cell body swelling (indicated by the diverging lines connecting the edges of the same cell before and after NMDA treatment) compared with the

scrambled shRNA control (Fig. 5, A–C). In neurons transfected with shRNA-GluN2Bm, there was a more dramatic reduction for the number of neurons with these pathological morphology changes (Fig. 5, A–C). Knockdown with another pair of shRNAs (i.e. shRNA-GluN2Ac and shRNA-GluN2Bi) showed the same effects (data not shown).

We next examined the effects of GluN2A and GluN2B knockdown on NMDAR-mediated deactivation of CREB. In neurons stimulated with 50  $\mu$ M NMDA, knockdown of GluN2A (by shRNA-GluN2Aa (Fig. 5D) and shRNA-GluN2Ac (data not shown)) or GluN2B (by shRNA-GluN2Bm (Fig. 5D) and shRNA-GluN2Bi (data not shown)) reversed the dephosphorylation of CREB. Consistent with the excitotoxicity data (Fig. 5, A–C), the attenuation of CREB dephosphorylation was significantly larger by the GluN2B shRNAs than the GluN2A shRNAs (Fig. 5D).

**Overexpression of GluN2A and GluN2B Exacerbates NMDAR-mediated Neuronal Death**—We next examined whether enhancing GluN2A and GluN2B function exacerbates NMDA-induced cell death. Neurons overexpressing GFP-GluN2A or GFP-GluN2B constructs, which were characterized previously and showed a similar function to those of endogenous GluN2A/2B subunits (24), were stimulated by 50  $\mu$ M NMDA on DIV 9. We chose DIV 9 neurons to examine the direct effect of GluN2A overexpression on neuronal death because the expression level of endogenous GluN2A was low and almost undetectable at this age (data not shown). In unstimulated naïve neurons, overexpression of the GluN2A or GluN2B subunits did not affect the basal level of p-CREB and neuronal death (data not shown). Interestingly, 50  $\mu$ M NMDA triggered more death in GFP-GluN2A- or GFP-GluN2B-transfected neurons when compared with the GFP-transfected neurons (Fig. 6A). Consistently, 50  $\mu$ M NMDA induced more dephosphorylation of CREB in GFP-GluN2A- or GFP-GluN2B-transfected neurons as compared with GFP-transfected neurons (Fig. 6B). It is also evident that overexpression of GluN2B had a larger impact on NMDA-triggered cell death and CREB deactivation than GluN2A. Taken together, our results demonstrate that GluN2A and GluN2B participate in both syn- and ex-NMDAR function as well as in the bidirectional regulation of cell fate.

## DISCUSSION

Although there is a consensus on the causal role of NMDAR overactivation in excitotoxicity following ischemic stroke, the functional involvement of particular subunits or subpopulations of NMDAR is not clear. GluN2A and GluN2B are the predominant GluN2 subunits in the adult forebrain. GluN2A- and GluN2B-containing NMDARs differ in channel kinetics, open probability, ligand affinity, and the interaction with intracellular signaling and scaffold proteins (14). Previous studies have demonstrated that GluN2A and GluN2B are expressed predominantly at the synapse and extrasynaptic locations, respectively (12, 13, 45, 46). Functionally, GluN2A-containing NMDARs mediated roughly 68% of the synaptic current and 27% of the extrasynaptic current. The remaining current at these distinct subcellular locations is mediated mainly by GluN2B (8). However, it is not known whether GluN2A and 2B differentially mediate certain intracellular signaling following

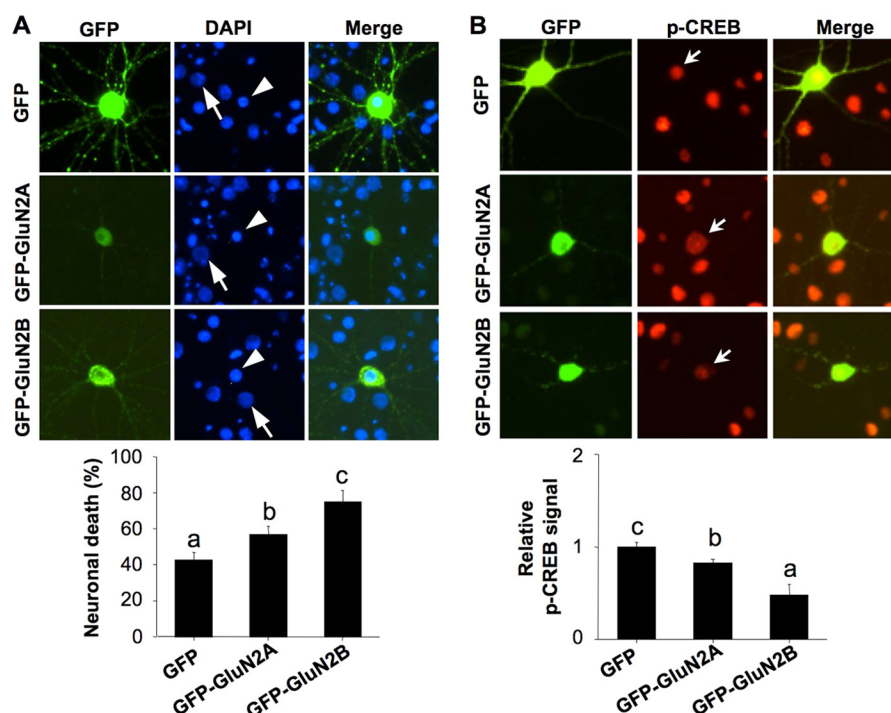


**FIGURE 6. Overexpression of GluN2A and GluN2B exaggerates NMDAR-induced cell death and CREB deactivation.** *A*, neurons transfected with a plasmid expressing GFP, GFP-GluN2A, or GFP-GluN2B were treated with 50  $\mu$ M NMDA for 30 min. Three hours later, neurons were fixed and costained with DAPI and antibody against GFP. Quantification of cell death, as revealed by condensed nuclear DAPI staining (arrowheads) in GFP-positive neurons, is shown in the bottom panel. Some of the healthy cells with diffuse nuclear staining are indicated by the arrows. *B*, neurons expressing GFP, GFP-GluN2A, or GFP-GluN2B were stimulated by 50  $\mu$ M NMDA for 15 min and then fixed and costained for p-CREB and GFP. The optical intensity of p-CREB (as indicated by arrows for the representative cells) in neurons transfected with GFP was defined as 1. One-way ANOVA revealed a significant difference (i.e.  $p < 0.05$ ) among different treatments. The post hoc SNK analysis revealed that the values associated with distinct SNK groups (*a*, *b*, and *c*) are significantly different:  $a < b < c$ .

syn- and ex-NMDAR activation. Here we found that activation of syn-NMDAR stimulated the prosurvival CREB-*Bdnf* cascade, which was suppressed significantly by inhibiting either GluN2A or GluN2B. This is consistent with both GluN2A and GluN2B regulating long-term potentiation (45, 47) and long-term depression (14, 48), which require syn-NMDAR function. Our data also suggest that the magnitude of NMDAR-mediated currents may not be related proportionally to the degree of intracellular signaling. For example, GluN2A activation had less of an effect than GluN2B on CREB up-regulation triggered by syn-NMDAR activation.

The prevailing theory on NMDAR-mediated excitotoxicity emphasizes that activation of syn-NMDAR supports cell survival and that activation of ex-NMDAR leads to cell death (9, 49). However, our recent study, along with others, demonstrated that activation of ex-NMDAR failed to shut off prosurvival signaling (17, 50) and did not trigger cell death (17, 51). It is interesting to note that certain types of neurons (such as retinal ganglion cells) only express ex-NMDAR and are resistant to glutamate-induced excitotoxicity (52). Further, 50  $\mu$ M NMDA, which is toxic to mature neurons, activates prosurvival signaling rather than causing death in young and developing neurons, which mainly express ex-NMDAR (53–55). Here, we confirmed that activation of ex-NMDAR alone up-regulated the CREB-*Bdnf* cascade and that such up-regulation depended on both GluN2A and GluN2B. Our data suggest that GluN2A and GluN2B expression at synaptic and extrasynaptic sites is functionally relevant to their involvement in activating CREB through both syn- and ex-NMDAR.

Several lines of evidence demonstrate that NMDAR bidirectionally regulates cell fate. Although appropriate NMDAR activity supports survival, overactivation turns off prosurvival signaling and triggers cell death. We found recently that the magnitude of excitotoxicity depends on the degree of syn- and ex-NMDAR coactivation (17). The fact that GluN2A and GluN2B are required for both synaptic and extrasynaptic signaling is consistent with the fact that the inhibition of these two subunits dampened NMDAR-mediated death. In support of our results, previous studies have also shown that GluN2B inhibition attenuates NMDA excitotoxicity, OGD-induced cell death, and ischemic stroke (7, 8, 56). It is important to note that, although preinsult GluN2B inhibition attenuates death, postinsult administration of the GluN2B antagonist may not be effective (57).

It is intriguing that several previous studies have mainly demonstrated the function of GluN2A in survival. When GluN2A is inhibited, either synaptic or extrasynaptic NMDAR activation leads to cell death. The NMDA-induced excitotoxicity is attenuated by the GluN2B antagonist but exaggerated (8) or not affected (56) by the GluN2A antagonist. The discrepancy between these two early studies and ours may be due to an important difference in experimental conditions. Compared with our experimental setup, these early studies did not include nifedipine (an antagonist for L-VGCCs) and CNQX (an antagonist for non-NMDA-type glutamate receptors) during NMDA stimulation. Because the activation of VGCCs (35–37, 43) and non-NMDA-type glutamate receptors (38–40) contributes significantly to excitotoxicity-induced  $\text{Ca}^{2+}$  overload, NMDA



stimulation without nifedipine and CNQX may impose a more severe pathological insult. It is possible that the protective effect from GluN2A inhibition may depend on the degree of the insults. Our data show that, following a more severe insult (such as stimulation with 100  $\mu$ M NMDA, Fig. 4A), inhibition of GluN2A by NVP-AAM077 did not attenuate cell death. Moreover, NVP-AAM077 attenuated NMDA-induced (at 50  $\mu$ M) CREB dephosphorylation (Figs. 1C and 4B) and cell death (Fig. 4A) when nifedipine and CNQX were included in the treatment. The protective effects from NVP-AAM077 were lost in the absence of nifedipine and CNQX (Fig. 4, C1 and C2). Consistently, NVP-AAM077 treatment resulted in stronger protective effects following a milder insult (e.g. stimulation with 30  $\mu$ M NMDA) (Fig. 4A). The fact that GluN2A knockout brain is more resistant to ischemia is in line with our conclusion (58). Other lines of evidence also suggest the function of GluN2A in neurodegeneration. For example, younger neurons (such as DIV 3–7 neurons), which lack significant GluN2A expression, are more tolerant to NMDA insults. Moreover, pharmacological inhibition of GluN2A significantly reduces excitotoxic  $\text{Ca}^{2+}$  overload in NMDA-stimulated neurons (43).

In summary, this study, for the first time, demonstrates that GluN2A and GluN2B regulate both synaptic and extrasynaptic signaling instead of displaying opposing functions. Mechanistically, inhibition of GluN2A and GluN2B may reduce cell death through the suppression of NMDAR-mediated CREB deactivation. Our data also demonstrate a larger impact of GluN2B than GluN2A on NMDAR-mediated intracellular signaling and excitotoxicity.

**Acknowledgments**—We thank Dr. Yves P. Auberson at the Novartis Institutes of Biomedical Research for providing NVP-AAM077 and Dr. Katherine Roche at the National Institute of Neurological Disorders and Stroke for providing the GFP-GluN2A and GFP-GluN2B constructs.

## REFERENCES

- Traynelis, S. F., Wollmuth, L. P., McBain, C. J., Menniti, F. S., Vance, K. M., Ogden, K. K., Hansen, K. B., Yuan, H., Myers, S. J., and Dingledine, R. (2010) Glutamate receptor ion channels. Structure, regulation, and function. *Pharmacol. Rev.* **62**, 405–496
- Benarroch, E. E. (2011) NMDA receptors. Recent insights and clinical correlations. *Neurology* **76**, 1750–1757
- Ikonomidou, C., Bosch, F., Miksa, M., Bittigau, P., Vöckler, J., Dikranian, K., Tenkova, T. I., Stefovskaya, V., Turski, L., and Olney, J. W. (1999) Blockade of NMDA receptors and apoptotic neurodegeneration in the developing brain. *Science* **283**, 70–74
- Lee, L. J., Lo, F. S., and Erzurumlu, R. S. (2005) NMDA receptor-dependent regulation of axonal and dendritic branching. *J. Neurosci.* **25**, 2304–2311
- Hunt, D. L., and Castillo, P. E. (2012) Synaptic plasticity of NMDA receptors. Mechanisms and functional implications. *Curr. Opin. Neurobiol.* **22**, 496–508
- Muir, K. W. (2006) Glutamate-based therapeutic approaches. Clinical trials with NMDA antagonists. *Curr. Opin. Pharmacol.* **6**, 53–60
- Chen, M., Lu, T. J., Chen, X. J., Zhou, Y., Chen, Q., Feng, X. Y., Xu, L., Duan, W. H., and Xiong, Z. Q. (2008) Differential roles of NMDA receptor subtypes in ischemic neuronal cell death and ischemic tolerance. *Stroke* **39**, 3042–3048
- Liu, Y., Wong, T. P., Aarts, M., Rooyackers, A., Liu, L., Lai, T. W., Wu, D. C., Lu, J., Tymianski, M., Craig, A. M., and Wang, Y. T. (2007) NMDA receptor subunits have differential roles in mediating excitotoxic neuronal death both *in vitro* and *in vivo*. *J. Neurosci.* **27**, 2846–2857
- Hardingham, G. E., and Bading, H. (2010) Synaptic versus extrasynaptic NMDA receptor signalling. Implications for neurodegenerative disorders. *Nat. Rev. Neurosci.* **11**, 682–696
- Forrest, D., Yuzaki, M., Soares, H. D., Ng, L., Luk, D. C., Sheng, M., Stewart, C. L., Morgan, J. I., Connor, J. A., and Curran, T. (1994) Targeted disruption of NMDA receptor 1 gene abolishes NMDA response and results in neonatal death. *Neuron* **13**, 325–338
- Monyer, H., Burnashev, N., Laurie, D. J., Sakmann, B., and Seeburg, P. H. (1994) Developmental and regional expression in the rat brain and functional properties of four NMDA receptors. *Neuron* **12**, 529–540
- Harris, A. Z., and Pettit, D. L. (2007) Extrasynaptic and synaptic NMDA receptors form stable and uniform pools in rat hippocampal slices. *J. Physiol.* **584**, 509–519
- Thomas, C. G., Miller, A. J., and Westbrook, G. L. (2006) Synaptic and extrasynaptic NMDA receptor NR2 subunits in cultured hippocampal neurons. *J. Neurophysiol.* **95**, 1727–1734
- Yashiro, K., and Philpot, B. D. (2008) Regulation of NMDA receptor subunit expression and its implications for LTD, LTP, and metaplasticity. *Neuropharmacology* **55**, 1081–1094
- Martel, M. A., Ryan, T. J., Bell, K. F., Fowler, J. H., McMahon, A., Al-Mubarak, B., Komiyama, N. H., Horsburgh, K., Kind, P. C., Grant, S. G., Wyllie, D. J., and Hardingham, G. E. (2012) The subtype of GluN2 C-terminal domain determines the response to excitotoxic insults. *Neuron* **74**, 543–556
- Tu, W., Xu, X., Peng, L., Zhong, X., Zhang, W., Soundarapandian, M. M., Balel, C., Wang, M., Jia, N., Zhang, W., Lew, F., Chan, S. L., Chen, Y., and Lu, Y. (2010) DAPK1 interaction with NMDA receptor NR2B subunits mediates brain damage in stroke. *Cell* **140**, 222–234
- Zhou, X., Hollern, D., Liao, J., Andrechek, E., and Wang, H. (2013) NMDA receptor-mediated excitotoxicity depends on the coactivation of synaptic and extrasynaptic receptors. *Cell Death Dis.* **4**, e560
- Zheng, F., Zhou, X., Luo, Y., Xiao, H., Wayman, G., and Wang, H. (2011) Regulation of brain-derived neurotrophic factor exon IV transcription through calcium responsive elements in cortical neurons. *PLoS ONE* **6**, e28441
- Nguyen, S. M., Lieven, C. J., and Levin, L. A. (2007) Simultaneous labeling of projecting neurons and apoptotic state. *J. Neurosci. Methods* **161**, 281–284
- Chen, K., Zhang, Q., Wang, J., Liu, F., Mi, M., Xu, H., Chen, F., and Zeng, K. (2009) Taurine protects transformed rat retinal ganglion cells from hypoxia-induced apoptosis by preventing mitochondrial dysfunction. *Brain Res.* **1279**, 131–138
- Goldberg, M. P., and Choi, D. W. (1993) Combined oxygen and glucose deprivation in cortical cell culture. Calcium-dependent and calcium-independent mechanisms of neuronal injury. *J. Neurosci.* **13**, 3510–3524
- Hasbani, M. J., Schlieff, M. L., Fisher, D. A., and Goldberg, M. P. (2001) Dendritic spines lost during glutamate receptor activation reemerge at original sites of synaptic contact. *J. Neurosci.* **21**, 2393–2403
- Zhou, X., Zheng, F., Moon, C., Schluter, O. M., and Wang, H. (2012) Bi-directional regulation of CaMKII $\alpha$  phosphorylation at Thr-286 by NMDA receptors in cultured cortical neurons. *J. Neurochem.* **122**, 295–307
- Sanz-Clemente, A., Matta, J. A., Isaac, J. T., and Roche, K. W. (2010) Casein kinase 2 regulates the NR2 subunit composition of synaptic NMDA receptors. *Neuron* **67**, 984–996
- Barneda-Zahonero, B., Servitja, J. M., Badiola, N., Miñano-Molina, A. J., Fadó, R., Saura, C. A., and Rodríguez-Alvarez, J. (2012) Nurr1 protein is required for N-methyl-D-aspartic acid (NMDA) receptor-mediated neuronal survival. *J. Biol. Chem.* **287**, 11351–11362
- Navon, H., Bromberg, Y., Sperling, O., and Shani, E. (2012) Neuroprotection by NMDA preconditioning against glutamate cytotoxicity is mediated through activation of ERK 1/2, inactivation of JNK, and by prevention of glutamate-induced CREB inactivation. *J. Mol. Neurosci.* **46**, 100–108
- Mabuchi, T., Kitagawa, K., Kuwabara, K., Takasawa, K., Ohtsuki, T., Xia, Z., Storm, D., Yanagihara, T., Hori, M., and Matsumoto, M. (2001) Phosphorylation of cAMP response element-binding protein in hippocampal neurons as a protective response after exposure to glutamate *in vitro* and



- ischemia *in vivo*. *J. Neurosci.* **21**, 9204–9213
28. Weitlauf, C., Honse, Y., Auberson, Y. P., Mishina, M., Lovinger, D. M., and Winder, D. G. (2005) Activation of NR2A-containing NMDA receptors is not obligatory for NMDA receptor-dependent long-term potentiation. *J. Neurosci.* **25**, 8386–8390
29. Berberich, S., Punnakal, P., Jensen, V., Pawlak, V., Seeburg, P. H., Hvalby, Ø., and Köhr, G. (2005) Lack of NMDA receptor subtype selectivity for hippocampal long-term potentiation. *J. Neurosci.* **25**, 6907–6910
30. Sheng, M., Cummings, J., Roldan, L. A., Jan, Y. N., and Jan, L. Y. (1994) Changing subunit composition of heteromeric NMDA receptors during development of rat cortex. *Nature* **368**, 144–147
31. Li, J. H., Wang, Y. H., Wolfe, B. B., Krueger, K. E., Corsi, L., Stocca, G., and Vicini, S. (1998) Developmental changes in localization of NMDA receptor subunits in primary cultures of cortical neurons. *Eur. J. Neurosci.* **10**, 1704–1715
32. Zhou, X., Xiao, H., and Wang, H. (2011) Developmental changes of TrkB signaling in response to exogenous brain-derived neurotrophic factor in primary cortical neurons. *J. Neurochem.* **119**, 1205–1216
33. Choi, D. W. (1988) Glutamate neurotoxicity and diseases of the nervous system. *Neuron* **1**, 623–634
34. Villmann, C., and Becker, C. M. (2007) On the hypes and falls in neuroprotection. Targeting the NMDA receptor. *Neuroscientist* **13**, 594–615
35. Sribnick, E. A., Del Re, A. M., Ray, S. K., Woodward, J. J., and Banik, N. L. (2009) Estrogen attenuates glutamate-induced cell death by inhibiting  $\text{Ca}^{2+}$  influx through L-type voltage-gated  $\text{Ca}^{2+}$  channels. *Brain Res.* **1276**, 159–170
36. Stanika, R. I., Villanueva, I., Kazanina, G., Andrews, S. B., and Pivovarova, N. B. (2012) Comparative impact of voltage-gated calcium channels and NMDA receptors on mitochondria-mediated neuronal injury. *J. Neurosci.* **32**, 6642–6650
37. Pizzi, M., Ribola, M., Valerio, A., Memo, M., and Spano, P. (1991) Various  $\text{Ca}^{2+}$  entry blockers prevent glutamate-induced neurotoxicity. *Eur. J. Pharmacol.* **209**, 169–173
38. Sattler, R., and Tymianski, M. (2001) Molecular mechanisms of glutamate receptor-mediated excitotoxic neuronal cell death. *Mol. Neurobiol.* **24**, 107–129
39. Frandsen, A., Drejer, J., and Schousboe, A. (1989) Direct evidence that excitotoxicity in cultured neurons is mediated via *N*-methyl-D-aspartate (NMDA) as well as non-NMDA receptors. *J. Neurochem.* **53**, 297–299
40. Brorson, J. R., Manzolillo, P. A., and Miller, R. J. (1994)  $\text{Ca}^{2+}$  entry via AMPA/KA receptors and excitotoxicity in cultured cerebellar Purkinje cells. *J. Neurosci.* **14**, 187–197
41. Szydlowska, K., and Tymianski, M. (2010) Calcium, ischemia and excitotoxicity. *Cell Calcium* **47**, 122–129
42. Xiong, Z. G., Zhu, X. M., Chu, X. P., Minami, M., Hey, J., Wei, W. L., MacDonald, J. F., Wemmie, J. A., Price, M. P., Welsh, M. J., and Simon, R. P. (2004) Neuroprotection in ischemia. Blocking calcium-permeable acid-sensing ion channels. *Cell* **118**, 687–698
43. Stanika, R. I., Pivovarova, N. B., Brantner, C. A., Watts, C. A., Winters, C. A., and Andrews, S. B. (2009) Coupling diverse routes of calcium entry to mitochondrial dysfunction and glutamate excitotoxicity. *Proc. Natl. Acad. Sci. U.S.A.* **106**, 9854–9859
44. Schlüter, O. M., Xu, W., and Malenka, R. C. (2006) Alternative N-terminal domains of PSD-95 and SAP97 govern activity-dependent regulation of synaptic AMPA receptor function. *Neuron* **51**, 99–111
45. Miwa, H., Fukaya, M., Watabe, A. M., Watanabe, M., and Manabe, T. (2008) Functional contributions of synaptically localized NR2B subunits of the NMDA receptor to synaptic transmission and long-term potentiation in the adult mouse CNS. *J. Physiol.* **586**, 2539–2550
46. Tovar, K. R., and Westbrook, G. L. (1999) The incorporation of NMDA receptors with a distinct subunit composition at nascent hippocampal synapses *in vitro*. *J. Neurosci.* **19**, 4180–4188
47. Sakimura, K., Kutsuwada, T., Ito, I., Manabe, T., Takayama, C., Kushiya, E., Yagi, T., Aizawa, S., Inoue, Y., and Sugiyama, H. (1995) Reduced hippocampal LTP and spatial learning in mice lacking NMDA receptor  $\epsilon$  1 subunit. *Nature* **373**, 151–155
48. Brigman, J. L., Wright, T., Talani, G., Prasad-Mulcare, S., Jinde, S., Seabold, G. K., Mathur, P., Davis, M. I., Bock, R., Gustin, R. M., Colbran, R. J., Alvarez, V. A., Nakazawa, K., Delpire, E., Lovinger, D. M., and Holmes, A. (2010) Loss of GluN2B-containing NMDA receptors in CA1 hippocampus and cortex impairs long-term depression, reduces dendritic spine density, and disrupts learning. *J. Neurosci.* **30**, 4590–4600
49. Hardingham, G. E., Fukunaga, Y., and Bading, H. (2002) Extrasynaptic NMDARs oppose synaptic NMDARs by triggering CREB shut-off and cell death pathways. *Nat. Neurosci.* **5**, 405–414
50. Gao, C., Gill, M. B., Tronson, N. C., Guede, A. L., Guzmán, Y. F., Huh, K. H., Corcoran, K. A., Swanson, G. T., and Radulovic, J. (2010) Hippocampal NMDA receptor subunits differentially regulate fear memory formation and neuronal signal propagation. *Hippocampus* **20**, 1072–1082
51. Wroge, C. M., Hogins, J., Eisenman, L., and Mennerick, S. (2012) Synaptic NMDA receptors mediate hypoxic excitotoxic death. *J. Neurosci.* **32**, 6732–6742
52. Ullian, E. M., Barkis, W. B., Chen, S., Diamond, J. S., and Barres, B. A. (2004) Invulnerability of retinal ganglion cells to NMDA excitotoxicity. *Mol. Cell Neurosci.* **26**, 544–557
53. Friedman, L. K., and Segal, M. (2010) Early exposure of cultured hippocampal neurons to excitatory amino acids protects from later excitotoxicity. *Int. J. Dev. Neurosci.* **28**, 195–205
54. Li, B., Chen, N., Luo, T., Otsu, Y., Murphy, T. H., and Raymond, L. A. (2002) Differential regulation of synaptic and extra-synaptic NMDA receptors. *Nat. Neurosci.* **5**, 833–834
55. Zhou, X., Moon, C., Zheng, F., Luo, Y., Soellner, D., Nuñez, J. L., and Wang, H. (2009) *N*-methyl-D-aspartate-stimulated ERK1/2 signaling and the transcriptional up-regulation of plasticity-related genes are developmentally regulated following *in vitro* neuronal maturation. *J. Neurosci. Res.* **87**, 2632–2644
56. von Engelhardt, J., Coserea, I., Pawlak, V., Fuchs, E. C., Köhr, G., Seeburg, P. H., and Monyer, H. (2007) Excitotoxicity *in vitro* by NR2A- and NR2B-containing NMDA receptors. *Neuropharmacology* **53**, 10–17
57. Kemp, J. A., and McKernan, R. M. (2002) NMDA receptor pathways as drug targets. *Nat. Neurosci.* **5**, 1039–1042
58. Morikawa, E., Mori, H., Kiyama, Y., Mishina, M., Asano, T., and Kirino, T. (1998) Attenuation of focal ischemic brain injury in mice deficient in the epsilon1 (NR2A) subunit of NMDA receptor. *J. Neurosci.* **18**, 9727–9732